

Structures and stability of metal-doped GenM (n = 9, 10) clusters

Wei Qin, Wen-Cai Lu, Lin-Hua Xia, Li-Zhen Zhao, Qing-Jun Zang, C. Z. Wang, and K. M. Ho

Citation: AIP Advances 5, 067159 (2015); doi: 10.1063/1.4923316

View online: http://dx.doi.org/10.1063/1.4923316

View Table of Contents: http://scitation.aip.org/content/aip/journal/adva/5/6?ver=pdfcov

Published by the AIP Publishing

Articles you may be interested in

Adsorption of alkali, alkaline-earth, simple and 3d transition metal, and nonmetal atoms on monolayer MoS2 AIP Advances **5**, 057143 (2015); 10.1063/1.4921564

First-principles study of the noble metal-doped BN layer

J. Appl. Phys. **109**, 084308 (2011); 10.1063/1.3569725

The melting curve of ten metals up to 12 GPa and 1600 K

J. Appl. Phys. 108, 033517 (2010); 10.1063/1.3468149

Spectrally tunable magnetic nanoparticles designed for distribution/recollection applications

J. Appl. Phys. 107, 09B327 (2010); 10.1063/1.3355900

Impact of the metal cathode and CsF buffer layer on the performance of organic light-emitting devices

J. Appl. Phys. 95, 5397 (2004); 10.1063/1.1707201





Structures and stability of metal-doped Ge_nM (n = 9, 10) clusters

Wei Qin,^{1,a} Wen-Cai Lu,^{1,2} Lin-Hua Xia,¹ Li-Zhen Zhao,¹ Qing-Jun Zang,¹ C. Z. Wang,³ and K. M. Ho³

¹Laboratory of Fiber Materials and Modern Textile, the Growing Base for State Key Laboratory, and College of Physics, Qingdao University, Qingdao, Shandong 266071, P. R. China

²State Key Laboratory of Theoretical and Computational Chemistry, Institute of Theoretical Chemistry, Jilin University, Changchun, Jilin 130021, P. R. China

³Department of Physics and Astronomy and Ames Laboratory-U.S. DOE and, Iowa State University, Ames, Iowa 50011, USA

(Received 11 May 2015; accepted 15 June 2015; published online 26 June 2015)

The lowest-energy structures of neutral and cationic Ge_nM (n = 9, 10; M = Si, Li, Mg, Al, Fe, Mn, Pb, Au, Ag, Yb, Pm and Dy) clusters were studied by genetic algorithm (GA) and first-principles calculations. The calculation results show that doping of the metal atoms and Si into Ge_9 and Ge_{10} clusters is energetically favorable. Most of the metal-doped Ge cluster structures can be viewed as adding or substituting metal atom on the surface of the corresponding ground-state Ge_n clusters. However, the neutral and cationic $FeGe_{9,10}$, $MnGe_{9,10}$ and Ge_{10} Al are cage-like with the metal atom encapsulated inside. Such cage-like transition metal doped Ge_n clusters are shown to have higher adsorption energy and thermal stability. Our calculation results suggest that $Ge_{9,10}$ Fe and Ge_9 Si would be used as building blocks in cluster-assembled nanomaterials because of their high stabilities. © 2015 Author(s). All article content, except where otherwise noted, is licensed under a Creative Commons Attribution 3.0 Unported License. [http://dx.doi.org/10.1063/1.4923316]

I. INTRODUCTION

There has been considerable interest in metal-doped semiconductor clusters since the observation of the reaction between metal atom and silicon in a supersonic jet to form metal atom doped silicon clusters by Beck in 1987. It was shown by photo fragment spectroscopy that metal-doped silicon clusters are more stable than pure silicon clusters of the same size. This discovery has stimulated a lot of theoretical and experimental studies on the metal-doped silicon clusters. For example, photoelectron spectroscopy was used to show that EuSi₁₂ is the smallest encapsulated cage structure among Eu-Si clusters. First-principles calculation showed that WSi₁₂ cluster exhibits high stability dues to its closed-shell electronic structure. Both anion photoelectron spectroscopy and theoretical calculations also indicated that Sc@Si₁₆ is very stable. Compared with pure silicon clusters, metal atom doping not only improves the stability of silicon clusters, but also greatly changes their electronic properties, such as superconductivity, magnetism, optical and other properties.

In contrast to the studies of metal doped silicon clusters, investigation of metal-doped germanium clusters are relatively few, with several studies focus on transition metal-doped germanium clusters. $^{20-22}$ For example, Debashis et al. reported the relative stability of Sc, Ti, and V encapsulating Ge_n clusters in the size range $n=14-20.^{21}$ They also calculated the electronic properties such as HOMO-LUMO gap, ionization potential, vertical detachment energy, and electron affinity in order to gain insights into the stability of the clusters. 21 Since germanium also is one of the important

^aEmail: qinw@qdu.edu.cn



semiconductor elements, it is of great interest to investigate in more detail regarding to the stability of Ge clusters upon doping by various metal atoms.

Searching for stable clusters has become one of the main subjects in cluster science; $^{23-26}$ because it can be used as building blocks in cluster-assembled nanomaterials for various applications. 27,28 It is well known that Ge_{10} and Ge_{9} , especially Ge_{10} are relatively stable clusters; and they can be used as building blocks in medium-sized Ge clusters, such as Ge_{34-44} . 29,30 In this paper, we performed a systematic study of the structures and stability of metal doped and Ge ideals Ge clusters by structure optimization using genetic algorithm and ab initio calculations. The lowest-energy structures of neutral and cationic Ge_nM (ge 10; ge 10; ge 10; ge 11 is ge 12 in this paper, we performed a systematic study of the structures and stability of metal doped and Ge 13 in this paper, we performed a systematic study of the structures and stability of metal doped and Ge 13 in this paper, we performed a systematic study of the structures and stability of metal doped and Ge 13 in this paper, we performed a systematic study of the structures and stability of metal doped and Ge 14 in this paper, we performed a systematic study of the structures and stability of metal doped and Ge 16 in this paper, we performed a systematic study of the structures and stability of metal doped and Ge 16 in this paper, we performed a systematic study of the structures and stability of metal doped and Ge 16 in this paper, we performed a systematic study of the structures and stability of metal doped and Ge 16 in this paper, we performed a systematic study of the structures and stability of metal doped and Ge 16 in this paper, we performed a systematic study of the structures and stability of metal doped and Ge 16 in this paper, we performed a systematic study of the structures and stability of metal doped and Ge 16 in this paper, we performed a systematic study of the structures and stability of metal doped and Ge 16 in this paper, we performed a systematic study of

II. COMPUTATIONAL METHODS

The low-energy structures of the clusters are searched by genetic algorithm in which the local structure relaxation and energy evaluation are performed using first-principles calculations based on density functional theory (DFT). Initial structures for the GA search are generated either randomly or manually based chemistry intuitions. The offspings in the GA search are generated by the cut-and-paste operation. The first-principles DFT calculations were carried out at the levels of PBE/PAW in VASP³¹ and PBE/DND in Dmol³ of Material Studios, respectively. In Materials Studio (MS) Package the DFT calculations were done with the all-electron DFT method compiled in DMol³ with a double numerical basis with d-polarization function (DND). The exchange-correlation energy was treated within the generalized gradient approximation (GGA) of the Perdew, Burke and Enzerhof (PBE) functional. Self-consistent calculations were done with a convergence criterion of 10⁻⁵ Hartree on the total energy, and the structures were fully optimized without any symmetry constraints and with a convergence criterion of 0.002 Hartree/A° on the forces. In the VASP calculation, we employed the Projector Augmented Wave (PAW) - PBE method with a plane wave (PW) basis set. The energy cutoff we used is 249.7 eV. The energy convergence criterion for the self-consistent electronic calculation is 10^{-5} eV and that for the structure relaxation it is 10^{-4} eV. Spin orbit coupling is also considered in the VASP calculations for all metal-doped (except the simple metal-doped and Si-doped) Ge_nM clusters.

III. RESULTS AND DISCUSSIONS

A. Geometries

Pure Ge clusters - Prior to the discussion of the structures of the metal-doped Ge clusters, it is worthwhile to review the structures of the pure Ge₉, Ge₁₀, and Ge₁₁ clusters. FIG. 1 shows several low-energy isomers of the Ge₉₋₁₁ clusters. Isomer **a** is the ground-state structure. Isomers **b** and **c** are frequently observed as building blocks in large Ge clusters. 29,30,32 Experiment 33 has confirmed that the Ge₁₀ cluster is a magic cluster, i.e., it is energetically more stable than Ge₉ and Ge₁₁ clusters. The geometric structures of the Ge₉₋₁₁ isomers shown in FIG. 1 will serve as references for our discussion of the structures of metal-doped clusters.

Doping by simple metal Li, Mg and Al atoms - FIG. 2 shows the geometric structures of neutral and cationic Ge_nM (n = 9, 10; M = Li, Mg and Al) clusters. Among these clusters, there are many similarities between Li and Mg doped structures, both in neutral and cationic cases. The neutral Ge_9M and $Ge_{10}M$ (M = Li and Mg) clusters can be viewed as adding a Li or Mg atom to the Ge_9 -b or Ge_{10} -b isomers shown in Fig. 1, respectively. Similarly, the cationic Ge_9Li^+ and Ge_9Mg^+ clusters are based on the Ge_9 -c isomer while $Ge_{10}Li^+$ and $Ge_{10}Mg^+$ are based on the Ge_{10} -a isomer. There are some small differences between $Ge_{10}Li$ and $Ge_{10}Mg$ and between Ge_9Li^+ and Ge_9Mg^+ where the metal atoms are added to the different sites of the Ge_n clusters.

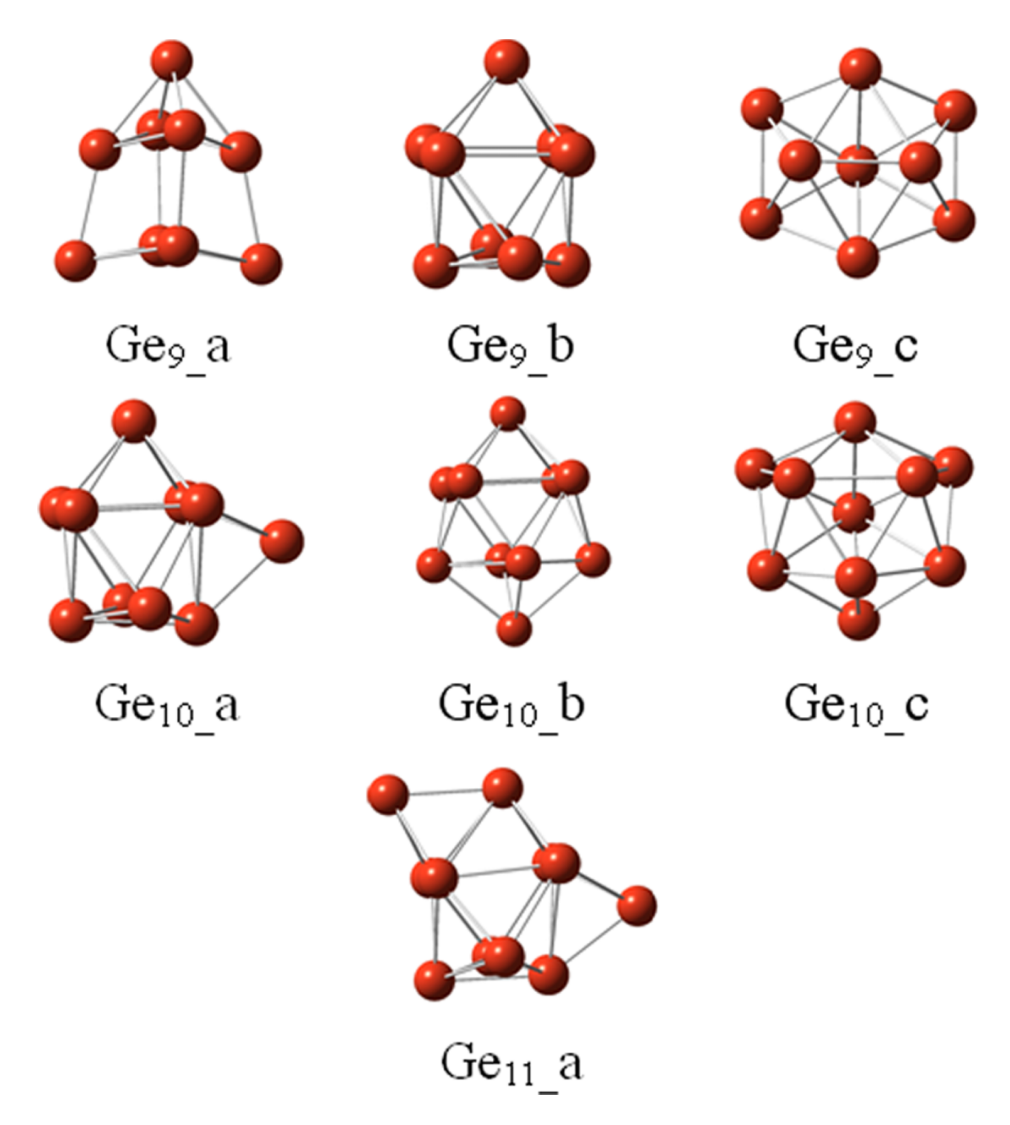


FIG. 1. Motifs of Ge_n (n = 9, 10) clusters. Isomers $\boldsymbol{a}, \boldsymbol{b}$ and \boldsymbol{c} are frequently observed as building blocks in Ge_nM clusters.

On the other hand, the structures of Al-doped clusters are different from those of Li or Mg doped clusters. Al atom trends to form more bonds with Ge upon doping. In particular, the $Ge_{10}Al$ cluster appears to be sphere-like. The Al atom is encapsulated in a cage formed by Ge atoms. This structure resembles the transition metal Fe and Mn doped clusters which will be discussed latter. For

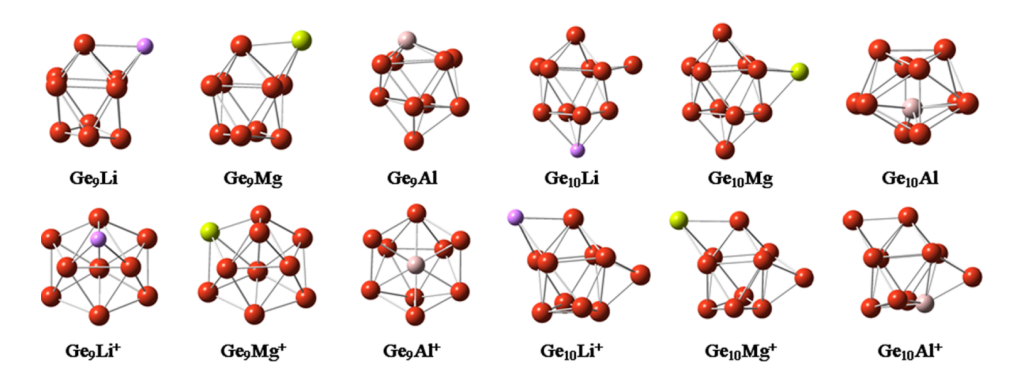


FIG. 2. Neutral and cationic geometric structures of Ge_9M and $Ge_{10}M$ (M=Li, Mg, and Al) clusters.

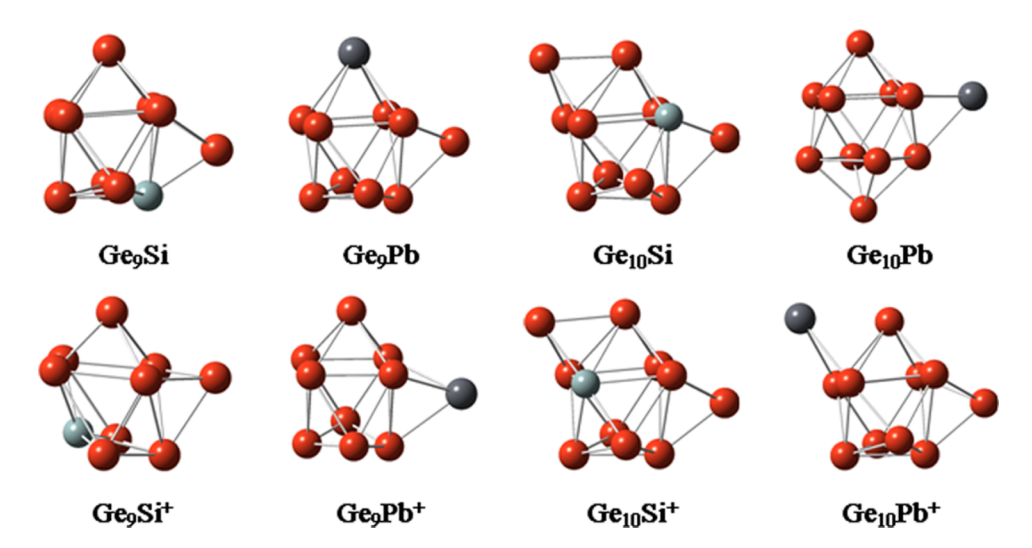


FIG. 3. Neutral and cationic geometric structures of Ge₉M and Ge₁₀M (M = Si and Pb) clusters.

Ge₉Al, Ge₉Al⁺ and Ge₁₀Al⁺ clusters, their configurations look like the structures of Ge₁₀**b**, Ge₁₀**c** and Ge₁₁a clusters, respectively; and Al atom tends to occupy the high coordination site in the clusters.

Doping by the same group elements Si and Pb - Si, Ge and Pb are the same group elements in periodic table of elements. Consequently, the geometries of both neutral and cationic Si-doped Ge_n clusters are the same as the ground-state structures of the corresponding pure Ge_{n+1} clusters, with a Si atom substituting a Ge atom at a high coordination site as shown in FIG. 3. For Pb atom doping, the structures of the neutral and cationic Ge_9Pb and cationic Ge_1Pb also adopt the ground-state geometries of Ge_{10} and Ge_{11} , but the Pb atom tends to cap on the Ge_n cluster and have low coordination; On the other hand, the neutral Ge_1Pb is formed by adding one Pb atom to Ge_1Db .

Doping by noble metals Au and Ag - FIG. 4 shows the structures of noble metal Au and Ag doped Ge_n clusters. While the neutral Ge_9Au cluster looks like a distorted Ge_{10} — \mathbf{a} , Ge_9Ag adopts the structure of Ge_{10} — \mathbf{c} , with a Ge atom being substituted by the Ag atom. Neutral $Ge_{10}Au$ and $Ge_{10}Ag$ clusters are formed by adding an Au or Ag atom to the Ge_{10} — \mathbf{b} and Ge_{10} — \mathbf{a} , but the metal atoms are attached at different sites. Au atom caps to the Ge-square at the bottom of Ge_{10} \mathbf{b} ; while Ag

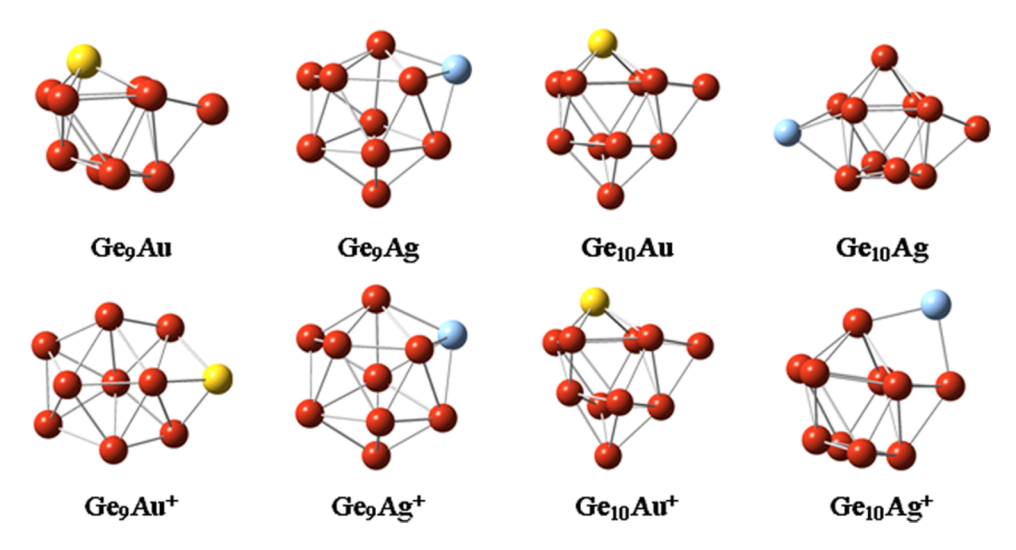


FIG. 4. Neutral and cationic geometric structures of Ge_9M and $Ge_{10}M$ (M = Au and Ag) clusters.

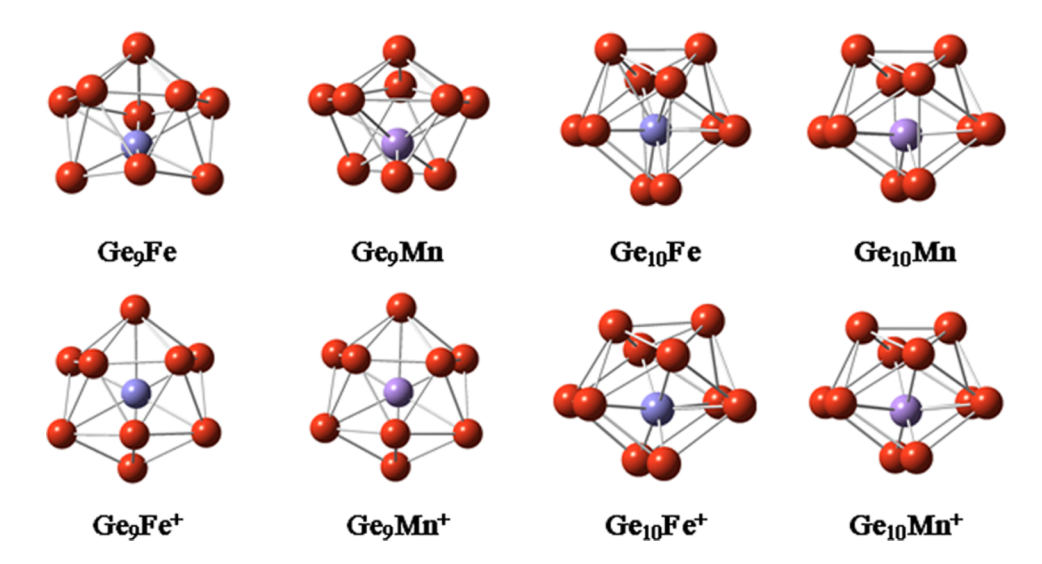


FIG. 5. Neutral and cationic geometric structures of Ge₉M and Ge₁₀M (M = Fe and Mn) clusters.

atom attaches to a side of the Ge triangle of the Ge_{10} **a**. For cationic Ge_nM clusters, the structures of the Ge_9Ag^+ and $Ge_{10}Au^+$ are similar to their corresponding neutral clusters, while Ge_9Au^+ and $Ge_{10}Ag^+$ are formed by adding an Au or Ag atom to the Ge_9 **c** and Ge_{10} **a** isomers, respectively.

Doping by transition metals Fe and Mn - The Fe and Mn doped Ge_9 and Ge_{10} clusters exhibit a cage motif with the metal atom encapsulated inside the cage as shown in FIG. 5. This motif is different from those in most of the other metal doped clusters discussed above except $Ge_{10}Al$ (see FIG. 2). In $Ge_{10}Al$, Al atom is also encapsulated inside a cage formed by Ge atoms, but the Al atom is not located close to the center of the cage. The structure of Ge_9Fe is similar to that of Ge_9Mn . The geometry of Ge_9Fe^+ is also the same as that of Ge_9Mn^+ . But the structures of the neutral and cationic Ge_9M (M=Fe, Mn) are not the same although all structures are cage like. On the other hand, the structures of both neutral and cationic Ge_1M (M=Fe, Mn) are very similar.

Doping by lanthanide metals Yb, Dy and Pm - For lanthanide we selected 3 metals: Yb with full filled 4f shell, Dy and Pm with some lone pair electrons. Similar to the case of doping by simple metals discussed above, most of the neutral and cationic Ge_9M clusters here can be viewed as adding one metal atom to the Ge_9 -b isomers as shown in FIG. 6 except Ge_9Pm^+ cluster. The structure of Ge_9Pm^+ does not resemble any structure motif of Ge_n clusters shown in Fig. 1. Ge_{10} Yb can be obtained by adding a Yb atom to Ge_{10} -b cluster. Ge_{10} Pm can also be obtained by adding a Pm atom to Ge_{10} -b but with more distortion. Ge_{10} Dy looks like a cage consists of several

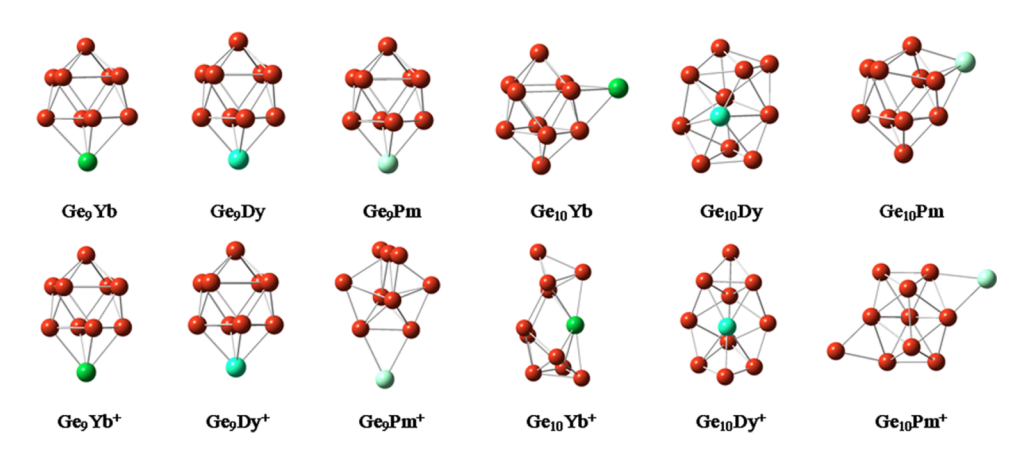


FIG. 6. Neutral and cationic geometric structures of Ge₉M and Ge₁₀M (M = Yb, Dy and Pm) clusters.

five-membered rings and a six-membered ring. The structures of the cationic $Ge_{10}M^+$ (M=Yb, Dy, and Pm) look peculiar. $Ge_{10}Yb^+$ is an elongated structure where a trigonal bipyramid and a pentagonal bipyramid are connected using the Yb atom as a common joint atom; $Ge_{10}Dy^+$ and $Ge_{10}Pm^+$ also do not simply follow the motifs of the pure Ge_n clusters.

B. Relative Stabilities

In order to gain a deeper insight into the thermal stability of the metal-doped Ge_9 and Ge_{10} clusters, we have studied the energy gain due to the metal adsorption on the Ge_9 and Ge_{10} clusters. The adsorption energy for a metal atom in a Ge_n cluster is defined as

$$E_{ads}(Ge_nM) = -[E_{tot}(Ge_nM) - E_{tot}(Ge_n) - E_a(M)]$$
(1)

Where $E_{ads}(Ge_nM)$, $E_{tot}(Ge_nM)$, $E_{tot}(Ge_n)$ and $E_a(M)$ are the adsorption energy of M on Ge_n , the total energy of the Ge_nM cluster, the total energy of the Ge_n cluster and the atomic energy of the metal atom, respectively. By this definition, the larger the E_{ads} , the more energy gain upon the formation of the metal-doped cluster thus the more stable of the Ge_nM cluster is. The calculations for the adsorption energies are performed using both the VASP at the level of PBE/PAW and the Dmol³ code in Material Studios at the level of PBE/DND. Spin polarization correction to the energy have also been considered in all the calculations.

The outputs of PBE/PAW of VASP give the total binding energy (E_b) of Ge_nM cluster which is defined as

$$E_b(Ge_nM) = E_{tot}(Ge_nM) - n*E_a(Ge) - E_a(M)$$
 (2)

Therefore, the adsorption energy can be calculated by the total binding energy of clusters in VASP, provide that the spin polarization effects in the atomic energies are included:

$$E_{ads}(Ge_nM) = -[E_b(Ge_nM) - E_b(Ge_n)]$$
(3)

However, in the binding energies calculated VASP, the atomic energies without spin polarization are used in the Eq. (2). Therefore, a correction to the atomic energy (E_{cor}) needs to be considered. Thus, the adsorption energy should be calculated by the formula below:

$$E_{ads}(Ge_nM) = -[E_b(Ge_nM) - E_b(Ge_n) - E_{cor}]$$
(4)

When the binding energies from the outputs of VASP are used, especially for transition metals where the spin polarization effects are significant. For many transition metals, the correction values have been provided by VASP.³⁴ In this work, the correction values (E_{cor}) are 3.15 eV for Fe and 5.62 eV for Mn, respectively.³⁴ For other metals where are correction values are not available from the VASP website we calculated their atomic energies with spin polarization $E_s(M)$ and without spin polarization $E_{ns}(M)$ in a big enough box. Then the E_{cor} is calculated by the differences of $E_s(M)$ and $E_{ns}(M)$, i.e. $E_{cor} = E_s(M) - E_{ns}(M)$.

The outputs of PBE/DND of Materials Studio (MS) provide both the total energy $E_{tot}(Ge_nM)$ and total binding energy $E_b(Ge_nM)$ of Ge_nM , and spin polarization is considered in atomic energies for binding energies calculation. Therefore, the atomic energies in the Dmol³ calculations can be determined using the outputs of total energies and binding energies. Then the adsorption energies can be calculated using Eq. (1).

The calculation results are shown in Table I and plotted in FIG. 7(a) and 7(b), respectively. The solid lines and dotted lines represent the adsorption energies for a metal atom in Ge₁₀ and Ge₉ clusters, respectively. From FIG. 7(a) we can see that all the metal-doped clusters studied in this paper are energetically stable with respect to the separated Ge_n cluster and a metal atom. In particular, Ge_n clusters doped with the same group Si and Pb atoms, transition metal Fe atom, and lanthanide metal Pm atom have relatively larger adsorption energies thus higher stability. The results of the PBE/DND in Dmol³ shown in FIG. 7(b) are enssentially consistent with the results from PBE/PAW calculation using VASP. One of the differences is that the stabilities of Ge_n clusters with Au doping in Dmol³ calculation are more stable than those in the VASP calculation. Furthermore,

TABLE I. Adsorption energies of Ge _n M (n = 9, 10; M = Li, Mg, Al, Si, Fe, Mn, Pb, Au, Ag, Yb, Pm and Dy) calculated	at
different level.	

Clusters	$E_{abs}(PBE/PAW)$	$E_{abs}(PBE/DND)$	Clusters	$E_{abs}(PBE/PAW)$	E _{abs} (PBE/DND)
Ge ₁₀ Li	1.7210	1.3747	Ge ₉ Li	2.1473	1.8659
$Ge_{10}Mg$	0.8220	0.4673	Ge ₉ Mg	1.1989	0.9577
Ge ₁₀ Al	2.4219	2.1950	Ge ₉ Al	3.1856	3.0691
Ge ₁₀ Si	2.9032	3.2413	Ge ₉ Si	4.7593	4.8396
Ge ₁₀ Fe	4.6520	4.7030	Ge ₉ Fe	5.0101	4.4331
$Ge_{10}Mn$	2.3980	2.6262	Ge ₉ Mn	4.0890	2.5632
Ge ₁₀ Pb	2.0806	1.7763	Ge ₉ Pb	3.4973	3.3596
Ge ₁₀ Au	1.7848	0.5094	Ge ₉ Au	2.2144	0.8970
Ge ₁₀ Ag	1.1593	0.8672	Ge ₉ Ag	1.5123	1.2576
Ge ₁₀ Yb	3.8298	1.7173	Ge ₉ Yb	4.4953	2.4376
Ge ₁₀ Pm	1.7054	3.8247	Ge ₉ Pm	2.1568	4.6014
Ge ₁₀ Dy	3.4638	3.4422	Ge ₉ Dy	4.4269	5.0067

the stability of Dy in the Ge₉ cluster is better in the PBE/DND as compared to PBE method in the VASP calculation.

We also found most of the Ge_9M clusters, particularly Ge_9Si , are more stable than the $Ge_{10}M$ clusters with the same M. This probably stem from the fact that Ge_{10} is a magic cluster. The transition metal Fe doping is special. Both Ge_9Fe and $Ge_{10}Fe$ have high stability. These results suggest that $Ge_{9,10}Fe$ and Ge_9Si would be used as building blocks for cluster-assembled nanomaterials.

We also calculated the binding energies per atoms of Ge₁₀M and Ge₉M clusters and the calculation results are plotted in FIG. 8. The binding energies are calculated using Eq. (2) and corrections to the atomic energies due to the spin polarization are included. The binding energy per atom of

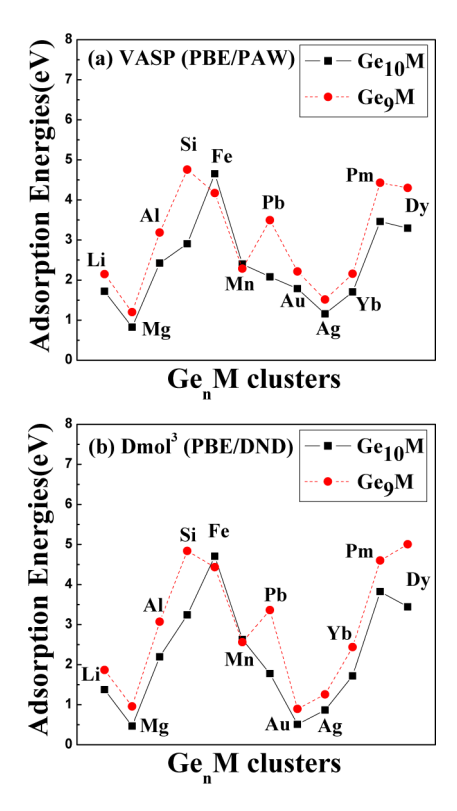


FIG. 7. Adsorption energies of Ge_nM calculated at two different levels. Solid lines and dash dots represent the adsorption energies of Ge_10M and Ge_9M calculated at the corresponding level, respectively.

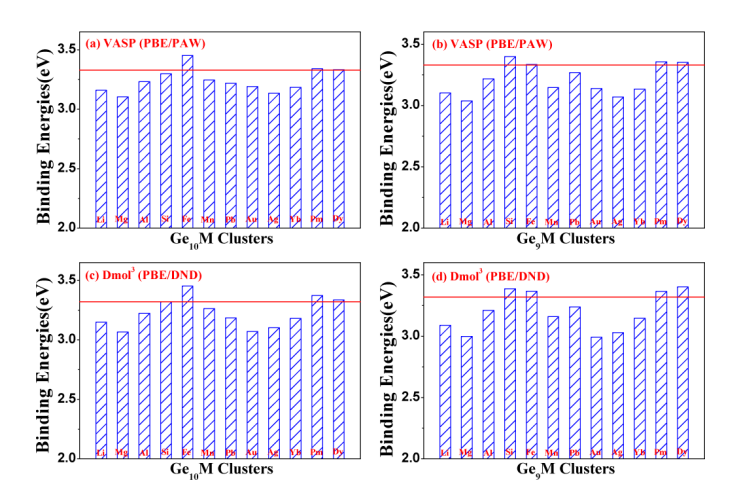


FIG. 8. Binding energies per atoms of $Ge_{10}M$ and $Ge_{9}M$ clusters at the level of PBE/PAW in VASP [(a) and (b)] and PBE/DND in Dmol³ [(c) and (d)]. Solid lines represent the binding energy per atoms of Ge_{10} magic cluster.

the Ge_{10} magic cluster is also shown as the solid red line in each plot for reference. The Ge_nM clusters with binding energy larger than Ge_{10} can be considered to be more stable than Ge_{10} . From FIG. 8 we can see the results of stability tend from both VASP and $Dmol^3$ calculations are very similar, although the energies from the $Dmol^3$ calculation exhibit larger variation. The calculation results also showed that stability of $Ge_{9,10}Fe$ and Ge_9Si are higher than Ge_{10} calculated from both codes. The clusters doping with Pm and Dy also have relatively higher stability. These results are consistent with the results from the adsorption energy analysis.

We next discuss the energy gap between the highest occupied (HOMO) and lowest unoccupied (LUMO) molecular orbitals of Ge_nM and Ge_{n+1} (n=9,10) clusters which are summarized in the Table II. The results show that the energy gaps of the clusters doped with Mg, Si, Pb, Au, Ag and Yb are relatively larger, while Pm and Mn doped clusters have smaller energy gaps. In general, clusters with larger HOMO-LUMO gaps exhibit high stability. However, adsorption energy and HOMO-LUMO gaps are not always strongly correlated. Comparing Table I and II, Ge_9Si has large adsorption energy, but relatively small HOMO-LUMO gap; while $Ge_{10}Mg$ have relatively small adsorption energy but large HOMO-LUMO gaps. The adsorption energy is related to the thermal stability of the cluster; and the HOMO-LUMO gap can be considered as a measure of chemical reaction stability of the cluster.

TABLE II. HOMO-LUMO Gaps (in eV) of Ge_nM and Ge_{n+1} (n = 9, 10; M = Li, Mg, Al, Si, Fe, Mn, Pb, Au, Ag Yb, Pm and Dy) calculated at the level of PBE/DND in Dmol³.

Clusters	HOMO-LUMO Gap	Clusters	HOMO-LUMO Gap
Ge ₁₀ Li	0.851	Ge ₉ Li	1.163
Ge ₁₀ Mg	1.559	Ge ₉ Mg	1.263
Ge ₁₀ Al	0.749	Ge ₉ Al	1.535
Ge ₁₀ Si	1.244	Ge ₉ Si	1.955
Ge ₁₀ Fe	1.257	Ge ₉ Fe	0.586
$Ge_{10}Mn$	0.314	Ge ₉ Mn	0.665
Ge ₁₀ Pb	1.001	Ge ₉ Pb	2.041
Ge ₁₀ Au	1.205	Ge ₉ Au	1.508
Ge ₁₀ Ag	1.004	Ge ₉ Ag	1.269
Ge ₁₀ Yb	1.546	Ge ₉ Yb	1.331
Ge ₁₀ Pm	0.34	Ge ₉ Pm	0.395
Ge ₁₀ Dy	1.181	Ge ₉ Dy	0.83
Ge ₁₁	1.266	Ge ₁₀	1.939

IV. CONCLUSIONS

The most stable structures of neutral and cationic Ge_nM (n=9,10; M is a metal atom including Li, Mg, Al, Fe, Mn, Pb, Au, Ag, Yb, Pm, Dy) and Ge_nSi clusters were studied at the DFT level with generalized gradient approximation in the form of PBE for exchange-correlation energy functional, using two different codes: VASP and Dmol³. Our calculation results show that most low-energy isomers of Ge_nM clusters are formed by adding the metal atom to the low-energy isomers of Ge_nM clusters. The transition metal Fe and Mn doped clusters are distinct from most of other clusters. Both the neutral and cationic Ge_nFe and Ge_nMn clusters are cage-like with the metal atom encapsulated inside the cage formed by Ge atoms. Energetic calculations show that such cage-like transition metal-doped Ge_n clusters have higher adsorption energy and thus higher thermal stability. And the clusters $Ge_{9,10}Fe$ and Ge_9Si may be used as building blocks in cluster-assembled nanomaterials because of their high stability.

ACKNOWLEDGMENTS

This work was supported by the China Postdoctoral Science Foundation (Grant No. 2014M561-885), the Postdoctoral Application Research Program of Qingdao of China and the National Natural Science Foundation of China (Grant No. 21273122). Li-Zhen Zhao acknowledges the support by the National Natural Science Foundation of China (Grant No. 21203105). Ames Laboratory is operated for the U.S. Department of Energy by Iowa State University under Contract No. DE-AC02-07CH11358. This work was also supported by the Director for Energy Research, Office of Basic Energy Sciences including a grant of computer time at the National Energy Research Supercomputing Center (NERSC) in Berkeley.

```
<sup>1</sup> S. M. Beck, J. Chem. Phys. 87, 4233 (1987).
 <sup>2</sup> H. Hiura, T. Miyazaki, and T. Kanayama, Phys. Rev. Lett. 86, 1733 (2001).
 <sup>3</sup> M. Ohara, K. Miyajima, A. Pramann, A. Makajima, and K. Kaya, J. Phys. Chem. A 106, 3702 (2002).
 <sup>4</sup> A. Grubisic, H. P. Wang, and Y. Ko, J. Chem. Phys. 129, 054302 (2008).
 <sup>5</sup> K. Koyasu, J. Atobe, and S. Furuse, J. Chem. Phys. 129, 214301 (2008).
 <sup>6</sup> V. Kumar and Y. Kawazoe, Phys. Rev. Lett. 87, 045503 (2001).
 <sup>7</sup> V. Kumar and Y. Kawazoe, Phys. Rev. B 65, 073404 (2000).
 <sup>8</sup> V. Kumar and Y. Kawazoe, Appl. Phys. Lett. 83, 2677 (2003).
 <sup>9</sup> H. J. W. Zandvliet, R. Van Moere, and B. Poelsema, Phys. Rev. B 68, 073404 (2003).
<sup>10</sup> H. Kawamura, V. Kumar, and Y. Kawazoe, Phys. Rev. B 70, 245433 (2004).
<sup>11</sup> H. Kawamura, V. Kumar, and Y. Kawazoe, Phys. Rev. B 71, 075423 (2005).
<sup>12</sup> A. K. Singh, V. Kumar, and Y. Kawazoe, Phys. Rev. B 71, 5429 (2005).
<sup>13</sup> S. N. Khanna, B. K. Rao, and P. Jena, Phys. Rev. Lett. 89, 6803 (2002).
<sup>14</sup> S. N. Khanna, B. K. Rao, P. Jena, and S. K. Nayak, Chem. Phys. Lett. 373, 433 (2003).
<sup>15</sup> J. Lu and S. Nagase, Phys. Rev. Lett. 90, 115506 (2003).
<sup>16</sup> P. Sen and L. Mitas, Phys. Rev. B 68, 155404 (2003).
<sup>17</sup> J. Q. Han and E. Hagelberg, Chem. Phys. 263, 255 (2001).
<sup>18</sup> J. Q. Han, C. Xiao, and F. Hagelberg, Struct. Chem. 13, 173 (2002).
<sup>19</sup> J. G. Han, Chem. Phys. 286, 181 (2003).
<sup>20</sup> V. Kumar, A. K. Singh, and Y. Kawazoe, Nano Lett. 4, 677 (2004).
<sup>21</sup> D. Bandyopadhyay, P. Kaur, and P. Sen, J. Phys. Chem. A 114, 12986 (2010).
<sup>22</sup> S. Neukermans, X. Wang, N. Veldeman, E. Janssens, R. E. Silverans, and P. Lievens, Inter. J. Mass Spec. 252, 145 (2006).
<sup>23</sup> X. Li, A. Grubisic, S. T. Stokes, J. Cordes, G. F. Gantefoer, K. H. Bowen, B. Kiran, M. Willis, P. Jena, R. Burgert, and H.
  Schnoeckel, Science 315, 356 (2007).
<sup>24</sup> D. E. Bergeron, P. J. Roach, A. W. Castleman, Jr., N. O. Jones, and S. N. Khanna, Science 307, 231 (2005).
<sup>25</sup> D. E. Bergeron, A. W. Castleman, Jr., T. Morisato, and S. N. Khanna, Science 304, 84 (2004).
<sup>26</sup> A. Ugrinov, A. Sen, A. C. Reber, M. Qian, and S. N. Khanna, J. Am. Chem. Soc. 130, 782 (2008).
<sup>27</sup> S. N. Khanna and P. Jena, Phys. Rev. Lett. 69, 1664 (1992).
<sup>28</sup> S. N. Khanna and P. Jena, Phys. Rev. B 51, 13705 (1995).
<sup>29</sup> W. Qin, W. C. Lu, L. Z. Zhao, Q. J. Zang, G. J. Chen, C. Z. Wang, and K. M. Ho, J. Chem. Phys. 131, 124507 (2009).
<sup>30</sup> W. Oin, W. C. Lu, O. J. Zang, L. Z. Zhao, G. J. Chen, C. Z. Wang, and K. M. Ho, J. Chem. Phys. 132, 214509 (2010).
<sup>31</sup> (a) G. Kresse, "Vienna ab initio simulation package, Technische Universitat Wien 1999 Hafner," J. Phys. Rev. B 47, 558
  (1993); (b) G. Kresse and Furthmuller, J. Phys. Rev. B 54, 11169 (1996).
<sup>32</sup> L. Z. Zhao, W. C. Lu, W. Qin, C. Z. Wang, and K. M. Ho, J. Phys. Chem. A 112, 5815 (2008).
<sup>33</sup> Q. L. Zhang, Y. Liu, R. F. Curl, F. F. Tittel, and R. E. Smalley, J. Chem. Phys. 88, 1670 (1988).
34 http://cms.mpi.univie.ac.at/vasp/vasp/Pseudopotentials_supplied_with_VASP_package.html.
```